Azastannatranes: Synthesis and Structural Characterization

Winfried Plass† and John G. Verkade*

Department of Chemistry, Iowa State University, Ames, Iowa 50011

Received March 3, 1993●

Syntheses of the new azastannatranes $ZSn(MeNCH_2CH_2)_3N$ (**5**, Z = *n*-Bu; **7**, Z = Me; **9**, Z = Ph; **11**, Z = Me_2N; **12**, Z = $^1/_2O$) and $ZSn(HNCH_2CH_2)_3N$ (**6**, Z = *n*-Bu; **8**, Z = Me; **10**, Z = Ph) are reported. Evidence for a pentacoordinate structure in these compounds is adduced from $^3J(^{119}SnH)$ couplings in the apical Z groups and from their ^{119}Sn chemical shifts measured in solution and in the solid state. In the case of **10**, two crystallographically different tin sites were suggested by ^{13}C and ^{119}Sn CP/MAS NMR spectroscopy. X-ray crystallographic experiments on this compound confirmed the presence of two trigonal bipyramidal structures featuring different $Sn–N_{ax}$ bond lengths (238.0(2), 245.3(2) pm). Crystal data: triclinic, $P\bar{1}$, a = 1089.6(2) pm, b = 1097.7(2) pm, c = 1356.9(3) pm, α = 107.80(1)°, β = 112.67(1)°, γ = 101.19(1)°, Z = 4, R = 0.031, R_w = 0.053. VT ^1H NMR spectral studies of **5–11** gave $\Delta G_{Tc}^{\ddagger}$ values ranging from 33.3 to 36.4 kcal/mol for the racemization of the rings in the triclinic cage moiety. Mass spectral and infrared features of **5–12** are also discussed.

Introduction

Atranes (**1**) have been extensively studied for a variety of M atoms and Z substituents, in particular for the group 14 elements Si, Ge, and Sn.[1] Azatranes (**2**) were quite rare (except for a few

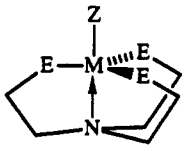

	E
1	O
2	NR
3	CH_2

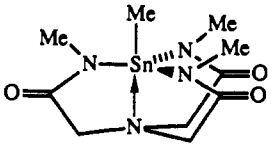

4

examples wherein M = Si)[2] until our recent expansion of this interesting class of compounds to include a broad variety of azasilatranes (Z = R, OR, NR_2),[3] and the first examples of azagermatranes,[4] azatitanatranes,[5] azavanadatranes (Z = O, NR),[6,7] azamolybdatranes (Z = N),[6] azaboratranes (Z = nothing),[8] azaalumatranes (Z = nothing),[8] and azaphosphatrane cations (Z = H^+).[9] The transition metal species $ZM(Me_3SiNCH_2CH_2)_3N$ (M = V, Ti; Z = Cl, R) and $M(t\text{-}BuMe_2SiNCH_2CH_2)_3N$ (M = Ti, V, Cr, Mn, Fe) were also recently described.[10] Although transannular dative Sn←N bonding has been observed in bicyclic and monocyclic azastannanes,[11] and also in stannatranes of types **1**[11c,e,12] and **3**,[11c,13] only one compound related to azastannatranes of type **2** has been reported, namely, **4**.[14] In contrast to stannatranes of type **1**, which were observed to bridge intermolecularly via their equatorial O atoms, the analogous NR groups in **4** apparently do not do so.[14a]

Aminostannanes are useful synthons in a variety of applications,[15] and recently we reported in a communication the utility of azastannatrane **5** in novel transmetalation reactions wherein azavanadatranes and azamolybdatranes were synthesized for the first time.[6] The latter azametallatranes failed to form in transamination reactions. Here we report the synthesis of **5–12**, the structure of **10** determined by X-ray means, and an investigation of the solid (^{13}C, ^{119}Sn) and solution (^1H, ^{13}C, ^{119}Sn) state NMR features of these compounds.

Experimental Section

All manipulations were carried out on a vacuum line with strict exclusion of moisture under an atmosphere of dry argon. Solvents were dried by standard methods[16] and distilled prior to use. IR and solid-state NMR

† New address: Fakultät für Chemie, Universität Bielefeld, Postfach 100131, 4800 Bielefeld 1, Germany.

● Abstract published in *Advance ACS Abstracts*, October 1, 1993.

(1) (a) Voronkov, M. G.; Baryshok, V. P. *J. Organomet. Chem.* **1982**, *239*, 199 and references therein. (b) Alder, R. W. *Acc. Chem. Res.* **1983**, *16*, 321 and references therein. (c) Hencsei, P.; Párkányi, L. *Rev. Silicon, Germanium, Tin and Lead Compd.* **1985**, *8*, 191 and references therein. (d) Kūpce, E.; Liepins, E.; Lapsina, A.; Zelcans, G.; Lukevics, *J. Organomet. Chem.* **1987**, *333*, 1 and references therein. (e) Stanislav, N.; Voronkov, M. G.; Alekseev, N. V. *Top. Curr. Chem.* **1986**, *131*, 99 and references therein.
(2) Lukevits, E.; Zelchan, E. I.; Solomenikova, I. I.; Liepins, E. E.; Yankovska, I. S.; Mazheika, I. B. *J. Gen. Chem. USSR (Engl. Transl.)* **1977**, *47*, 98.
(3) (a) Gudat, D.; Daniels, L. M.; Verkade, J. G. *J. Am. Chem. Soc.* **1989**, *111*, 8520. (b) Gudat, D.; Verkade, J. G. *Organometallics* **1989**, *8*, 2772. (c) Gudat, D.; Daniels, L. M.; Verkade, J. G. *Organometallics* **1990**, *9*, 1464. (d) Woning, J.; Daniels, L. M.; Verkade, J. G. *J. Am. Chem. Soc.* **1990**, *112*, 4601. (e) Gudat, D.; Verkade, J. G. *Organometallics* **1990**, *29*, 2172. (f) Woning, J.; Verkade, J. G. *J. Am. Chem. Soc.* **1991**, *113*, 944. (g) Woning, J.; Verkade, J. G. *Organometallics* **1991**, *10*, 2259.
(4) Wan, Y.; Verkade, J. G. *Inorg. Chem.* **1993**, *32*, 79.
(5) (a) Naiini, A.; Menge, W.; Verkade, J. G. *Inorg. Chem.* **1991**, *30*, 5009. (b) Naiini, A.; Ringrose, S. L.; Su, Y.; Jacobson, R. A.; Verkade, J. G. *Inorg. Chem.* **1993**, *32*, 1290.
(6) Plass, W.; Verkade, J. G. *J. Am. Chem. Soc.* **1992**, *114*, 2275.
(7) Plass, W.; Verkade, J. G. *Inorg. Chem.*, following paper in this issue.
(8) Pinkas, J.; Gaul, B.; Verkade, J. G. *J. Am. Chem. Soc.*, in press.
(9) (a) Lensink, C.; Xi, S.-K.; Daniels, L. M.; Verkade, J. G. *J. Am. Chem. Soc.* **1989**, *111*, 3478. (b) Laramay, M. A. H.; Verkade, J. G. *J. Am. Chem. Soc.* **1990**, *112*, 9421. (c) Laramay, M. A. H.; Verkade, J. G. *Z. Anorg. Allg. Chem.* **1991**, *605*, 163. (d) Verkade, J. G. *Phosphorus Chemistry in America-1991*; ACS Symposium Series 486; American Chemical Society: Washington, DC, 1992; Chapter 5, p 64. (e) Tang, J.; Laramay, M. A. H.; Verkade, J. G. *J. Am. Chem. Soc.* **1992**, *114*, 3129.
(10) (a) Cummins, C. C.; Schrock, R. R.; Davis, W. M. *Organometallics* **1992**, *11*, 1452. (b) Cummins, C. C.; Lee, J.; Schrock, R. R.; Davis, *Angew. Chem.* **1992**, *104*, 1510.
(11) (a) Mügge, C.; Jurkschat, K.; Tzschach, A.; Zschunke, A. *J. Organomet. Chem.* **1979**, *164*, 135. (b) Dräger, M. *J. Organomet. Chem.* **1983**, *251*, 209. (c) Tzschach, A.; Jurkschat, K. *Pure Appl. Chem.* **1986**, *58*, 639. (d) Schmidt, M.; Dräger, M.; Jurkschat, K. *J. Organomet. Chem.* **1991**, *410*, 43 and references therein. (e) Tzschach, A.; Jurkschat, K. *Comments Inorg. Chem.* **1983**, *3*, 35 and references therein. (f) Jastrzebski, J. T. B. H.; Boersma, J.; Esch, P. M.; van Koten, G. *Organometallics* **1991**, *10*, 930 and references therein.
(12) (a) Voronkov, M. G. *Pure Appl. Chem.* **1966**, *13*, 35 and references therein. (b) Zeldin, M.; Ochs, J. *J. Organomet. Chem.* **1975**, *86*, 369. (c) Jurkschat, K.; Mügge, C.; Tzschach, A.; Zschunke, A. *Z. Anorg. Allg. Chem.* **1980**, *463*, 123 and references therein.
(13) Jurkschat, K.; Tzschach, A. *J. Organomet. Chem.* **1984**, *272*, C13.
(14) (a) Tzschach, A.; Jurkschat, K.; Mügge, C. *Z. Anorg. Allg. Chem.* **1982**, *492*, 135. (b) Jurkschat, K. Dissertation, Martin-Luther-Universität Halle-Wittenberg, Germany, 1980.
(15) Lappert, M. F.; Power, P. P.; Sauger, A. R.; Srivastava, R. C. *Metal and Metalloid Amides*; John Wiley & Sons: New York, Chichester, Brisbane, Toronto, 1980.
(16) Perrin, D. D.; Armarego, W. L. F. *Purification of Laboratory Chemicals*, 3rd ed.; Pergamon Press: Oxford, New York, Frankfurt, 1988.

0020-1669/93/1332-5145$04.00/0

Table I. Synthesis Data for **5–11**

	R–$(NMe_2)_3$		$(R'–NHCH_2CH_2)_3N$							
cmpd	R	amt (g)	R′	amt (g)	amt of toluene (mL)	T (°C)	t (h)	distillation (°C, torr)	mp (°C)	yield (%)
5	*n*-Bu	41.50	Me	25.37	200	90	4	119–20, 0.01		90
6	*n*-Bu	8.47	H	4.02	60	80	2	118, 0.01		70
7	Me	6.10	Me	4.32	50	*a*	2.5	112, 0.5	70–71	90
8	Me	6.10	H	3.35	50[b]	*a*	1.5	*c*	109–110	64
9	Ph	6.52	Me	3.75	50	90	2	*c*	137	60
10	Ph	3.72	H	1.66	50	90	2	*c*	78	90
11	Me_2N	24.60	Me	15.70	250	100	5	*c*	81–82	81

[a] Reflux. [b] Reaction was slightly exothermic at first. [c] Recrystallized from toluene.

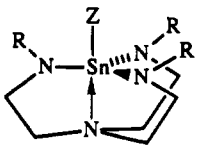

	Z	R		Z	R
5	*n*-Bu	Me	**9**	Ph	Me
6	*n*-Bu	H	**10**	Ph	H
7	Me	Me	**11**	Me_2N	Me
8	Me	H	**12**	1/2 O	Me

samples were prepared in a drybox under an atmosphere of dry and oxygen-free nitrogen. $(MeNCH_2CH_2)_3N$ (Me-tren) was prepared from tren using a previously published procedure.[17] Tetrakis(dimethylamino)stannane,[18,19] *n*-butyltris(dimethylamino)stannane,[18,19] tris(dimethylamino)phenylstannane,[18,19] and tris(dimethylamino)methylstannane[19] were prepared according to published procedures. Solution NMR spectra were recorded on Varian VXR 300 (^{1}H, 299.95 MHz; ^{13}C, 75.43 MHz; ^{119}Sn, 111.86 MHz) and Bruker WM 200 (^{113}Sn, 74.63 MHz) instruments using deuterated solvents as internal lock, and TMS (^{1}H, ^{13}C) or $SnMe_4$ (^{119}Sn) as external standards. As a solvent for low-temperature experiments, toluene-d_8 was used. Temperature calibration of the NMR spectra was carried out by literature methods.[20] For the acquisition of solid-state NMR spectra, polycrystalline samples (ca. 300–400 mg) were packed in either an airtight insert or directly into the rotor which was sealed with a threaded Teflon plunger. Solid-state NMR spectra were obtained on a Bruker MSL 300 spectrometer (^{119}Sn, 111.92 MHz; ^{13}C, 75.47 MHz) under proton decoupling using the CP-MAS technique. A 90° pulse was employed with mixing times for polarization transfer of 2–3 ms followed by a 6-s recycle delay. Spinning rates were in the range of 3–4.5 kHz. Generally, spectra were rerun at a different speed to establish the position of the center band. The magic angle was set by using the ^{79}Br resonance of KBr.[21] A sample of glycine (^{13}C) or tetracyclohexylstannane (^{119}Sn),[22] respectively, was used to set the Hartmann–Hahn matching condition.

Mass spectra were recorded on a Kratos MS50 (70 eV, EI) mass spectrometer, and high-resolution data were obtained by peak matching. IR spectra were recorded on an IBM 98 FT-IR spectrometer. Solid samples were measured as KBr pellets (4000–600 cm^{-1}) and as Nujol mulls between polyethylene plates (650–150 cm^{-1}), respectively, whereas liquid samples were measured neat between CsBr (4000–650 cm^{-1}) and polyethylene (650–150 cm^{-1}) plates. Melting points were determined by a Thomas-Hoover capillary melting point apparatus and are uncorrected. Microanalyses were carried out by Galbraith Laboratories, Knoxville, TN.

General Procedure for 5–11. An equimolar quantity of $(R'NHCH_2CH_2)_3N$ (Table I) was added to $RSn(NMe_2)_3$ in toluene. The reaction mixture was heated with stirring, and then the volatiles were removed in vacuo to give a residue which was vacuum-distilled or recrystallized from toluene. Yields were calculated after purification. Elemental analyses, mass spectral data, and infrared data appear in the supplementary material.

Bis(1-*N,N′,N″*-trimethylazastannatranyl) Oxide (12). When the reaction mixture for the preparation of compound **11** was exposed to traces of atmospheric moisture (via a 20-gauge needle through the septum) for 24 h, a colorless precipitate was formed. The toluene was removed in vacuo, and the residue was washed with three portions of diethyl ether, affording 1.62 g (65%) of pure **12** (mp dec >245 °C). Anal. Calcd (found) for $C_{18}H_{42}H_8OSn_2$: C, 34.65 (34.54); H, 6.78 (6.96); N, 17.96 (17.07). MS (EI, 70 eV): m/e 619.14511, 0.2% (calcd for $C_{18}H_{41}N_8O^{116}Sn^{118}Sn$ (M^+ – H), 619.14424); 439, 100% ((M^+ – 3×$CH_2N(CH_2)_2$ – Me – H) for $^{120}Sn^{120}Sn$); 305, 77% ($^1/_2$(M^+ – O) for ^{120}Sn). Infrared data: 273 (w), 307 (w), 395 (vw), 427 (vw), 506 (m), 566 (m, br), 595 (vw), 714 (sh), 748 (m), 814 (vs, br), 845 (s), 881 (vw), 926 (m), 1020 (vs), 1045 (vs), 1067 (m), 1111 (s), 1136 (vs, br), 1202 (vs), 1242 (m), 1281 (s), 1340 (m), 1352 (s), 1375 (w), 1414 (w), 1445 (vs), 1460 (sh), 1472 (m), 2665 (s), 2775 (vs, br), 2822 (vs, br), 2901 (vs), 2961 (vs) cm^{-1}.

Table II. Crystal Data for 1-Phenylazastannatrane (**10**)

formula	$C_{12}H_{20}N_4Sn$
fw	339.01
space group	$P\bar{1}$
a (pm)	1089.6(2)
b (pm)	1097.7(2)
c (pm)	1356.9(3)
α (deg)	107.80(1)
β (deg)	112.61(1)
γ (deg)	101.19(1)
V (10^{-30} m^3)	1333.9
Z	4
ρ_{calc} (10^3 kg m^{-1})	1.688
μ(Mo Kα) (m^{-1})	1907.0
scan method	θ–2θ
data collcn range, 2θ (deg)	4.0–50.0
tot. no of data	9335
tot. no of unique data	4668
no. of obsd data, with $F_o^2 > 3\sigma(F_o^2)$	4202
no. of parameters refined	808
data collcn instrument	Enraf-Nonius CAD4
temp (K)	198(1)
R^a	0.031
R_w^b	0.053
quality-of-fit parameter[c]	1.95
largest peak (10^{30} e/m^3)	0.8

[a] $R = \sum||F_o| - |F_c||\sum|F_o|$. [b] $R_w = [\sum w(|F_o| - |F_c|)^2/\sum w|F_o|^2]^{1/2}$; $w = 1/\sigma^2(|F_o|)$. [c] Quality-of-fit $= [\sum w(|F_o| - |F_c|)^2/(N_{observns} - N_{params})]^{1/2}$.

Crystal and Molecular Structure Determination for 1-Phenylazastannatrane (10). An entire sphere of data was collected at –75 °C on a colorless crystal mounted on the tip of a glass fiber. The cell constants were determined from a list of reflections found by an automated search routine. Pertinent data collection and reduction information is given in Table II. Lorentz and polarization corrections were applied. Intensity standards indicated an overall decay of 4.9%, so a linear correction was applied. An absorption correction was made, based on a series of azimuthal scans for several reflections having a Eulerian angle χ near 90°. Intensity statistics suggested the choice of the centric triclinic space group. The choice was verified by successful solution and refinement in space group $P\bar{1}$. The positions of the Sn atoms and the atoms in the coordination sphere were taken from a direct methods E map.[23] Following full-matrix refinement of these 12 atoms and application of a scaling factor, a subsequent difference Fourier map indicated the positions of the remainder of the non-hydrogen atoms. In the final stages of refinement, all non-hydrogen atoms were given anisotropic temperature factors. Hydrogen atoms were placed in idealized positions 0.95 Å from the carbon atom only and were used in the structure factor calculations but were not refined. Isotropic temperature factors for the hydrogen atoms were set at 130% of the isotropic equivalent of the corresponding carbon atom. Refinement calculations were performed on a Digital Equipment Corp. MicroVAX II computer using the CAD4-SDP programs.[24] The positional

(17) Dannley, M. L.; Lukin, M. *J. Org. Chem.* **1955**, *20*, 92.
(18) Jones, K.; Lappert, M. F. *J. Chem. Soc.* **1965**, 1944.
(19) Lorberth, J. *J. Organomet. Chem.* **1969**, *16*, 235.
(20) Martin, M. L.; Delpuech, J. J.; Martin, G. J. *Practical NMR Spectroscopy*; Heyden: London, 1980.
(21) Frye, J. S.; Maciel, G. E. *J. Magn. Reson.* **1982**, *48*, 125.
(22) Harris, R. K.; Sebald, A. *Magn. Reson. Chem.* **1987**, *25*, 1058.
(23) Sheldrick, G. M. SHELXS-86. Institute für Anorganische Chemie der Universität, Göttingen, Germany.

Table III. Positional Parameters and B(eq) Values for 1-Phenylazastrannatrane (**10**)

atom	x	y	z	B(eq)[a]
Sn(1)	0.09333(2)	0.24126(2)	0.4783492)	2.063(5)
Sn(2)	−0.30417(2)	−0.06777(2)	−0.02380(2)	1.769(5)
N(1)	0.2792(3)	0.2687(3)	0.4267(2)	2.30(6)
N(2)	0.2657(3)	0.2728(3)	0.6297(2)	3.04(7)
N(3)	0.0138(3)	0.0580(3)	0.3308(2)	2.50(7)
N(4)	0.0953(3)	0.4077(3)	0.4402(3)	3.39(8)
N(5)	−0.4067(3)	−0.3027(3)	−0.0510(2)	2.00(6)
N(6)	−0.4956(3)	−0.1365(3)	−0.1704(2)	2.62(7)
N(7)	−0.1704(3)	−0.1616(3)	−0.0602(2)	2.58(6)
N(8)	−0.3067(3)	−0.0359(3)	0.1336(2)	2.19(6)
C(1)	0.3932(4)	0.2572(4)	0.619893)	2.96(9)
C(2)	0.4112(4)	0.3236(4)	0.5395(3)	2.90(9)
C(3)	0.0948(4)	0.0566(3)	0.2653(3)	2.54(8)
C(4)	0.2537(3)	0.1310(4)	0.3445(3)	2.77(8)
C(5)	0.2190(4)	0.4738(4)	0.4329(3)	3.15(9)
C(6)	0.2658(4)	0.3667(4)	0.3730(3)	2.83(8)
C(7)	−0.0730(3)	0.2139(3)	0.5271(3)	2.25(7)
C(8)	−0.2158(4)	0.1565(4)	0.4406(3)	2.87(8)
C(9)	−0.3239(4)	0.1368(4)	0.4713(4)	3.6(1)
C(10)	−0.2890(4)	0.1741(4)	0.5881(3)	3.55(9)
C(11)	−0.1499(4)	0.2301(4)	0.6741(3)	3.50(9)
C(12)	−0.0413(4)	0.2526(4)	0.6446(3)	2.95(8)
C(13)	−0.5696(4)	−0.2850(4)	−0.2259(3)	3.14(9)
C(14)	−0.5578(4)	−0.3480(4)	−0.1389(3)	2.86(9)
C(15)	−0.1733(3)	−0.2853(3)	−0.0386(3)	2.81(8)
C(16)	−0.3265(4)	−0.3787(3)	−0.0938(3)	2.71(8)
C(17)	−0.3989(3)	−0.155993)	−0.1290(3)	2.55(7)
C(18)	−0.3855(3)	−0.2902(3)	0.0648(3)	2.57(8)
C(19)	−0.2139(3)	0.1436(3)	0.0076(3)	2.27(7)
C(20)	−0.1382(3)	0.2441(3)	0.1226(3)	2.55(8)
C(21)	−0.0928(4)	0.3809(3)	0.1461(3)	2.87(9)
C(22)	−0.1229(4)	0.4214(3)	0.054(3)	3.00(8)
C(23)	−0.1975(4)	0.3236(3)	−0.0594(3)	3.04(8)
C(24)	−0.2422(3)	0.1851(3)	−0.0831(3)	2.55(7)

[a] In units of $10^4 \times$ pm.^{2} Anisotropically refined atoms are given in the form of the isotropic equivalent displacement parameter defined as $(4/3)[a^2B(1,1) + b^2B(2,2) + c^2B(3,3) + ab(\cos\gamma)B(1,2) + ac(\cos\beta)B(1,3) + bc(\cos\alpha)B(2,3)]$.

Table IV. Selected Bond Distances and Angles for the Two Independent Molecules in 1-Phenylazastannatrane (**10**)

Bond Distances (pm)			
Sn(1)–N(1)	238.0(2)	Sn(2)–N(5)	245.3(2)
Sn(1)–N(2)	205.3(3)	Sn(2)–N(6)	203.9(2)
Sn(1)–N(3)	208.2(2)	Sn(2)–N(7)	206.2(2)
Sn(1)–N(4)	204.4(2)	Sn(2)–N(8)	206.8(2)
Sn(1)–C(7)	215.5(3)	Sn(2)–C(19)	217.3(3)
Bond Angles (deg)			
N(1)–Sn(1)–C(7)	178.75(9)	N(5)–Sn(2)–C(19)	177.43(9)
N(1)–Sn(1)–N(2)	78.01(9)	N(5)–Sn(2)–N(6)	78.49(9)
N(1)–Sn(1)–N(3)	78.79(8)	N(5)–Sn(2)–N(7)	76.22(8)
N(1)–Sn(1)–N(4)	77.14(9)	N(5)–Sn(2)–N(8)	78.17(8)
N(2)–Sn(1)–N(3)	118.5(1)	N(6)–Sn(2)–N(7)	110.0(1)
N(2)–Sn(1)–N(4)	115.3(1)	N(6)–Sn(2)–N(8)	117.1(1)
N(3)–Sn(1)–N(4)	113.5(1)	N(7)–Sn(2)–N(8)	118.51(9)
N(2)–Sn(1)–C(7)	101.0(1)	N(6)–Sn(2)–C(19)	102.5(1)
N(3)–Sn(1)–C(7)	101.06(9)	N(7)–Sn(2)–C(19)	105.45(9)
N(4)–Sn(1)–C(7)	104.0(1)	N(8)–Sn(2)–C(19)	99.28(9)
C(2)–N(1)–C(4)	113.6(2)	C(14)–N(5)–C(16)	113.5(2)
C(2)–N(1)–C(6)	112.7(2)	C(14)–N(5)–C(18)	113.7(2)
C(4)–N(1)–C(6)	113.5(2)	C(16)–N(5)–C(18)	113.7(2)

parameters and selected bond distances and angles are listed in Tables III and IV, respectively.

Results and Discussion

Syntheses. Transamination reactions of the group 14 elements Si, Ge, and Sn[15] occur more readily progressing down the group.[25] Thus formation of **5–11** from the corresponding tris(dimethylamino)stannanes by transamination with tren or Me-tren generally proceeds at room temperature in the absence of catalyst, although increasing the reaction temperature results in shorter reaction

$$Z\text{-}Sn(NMe_2)_3 + (HNRCH_2CH_2)_3N \xrightarrow{\text{toluene}}$$

Z = *n*-Bu, Me, Ph, Me_2N R = H (tren) R = Me (Me-tren)

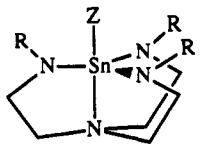

$+ 3HNMe_2$ (1)

5-11

times and higher yields. Even at high concentrations of the reactants, no formation of oligomeric or polymeric materials was observed. The azastannatranes **5–11** are all colorless solids or liquids and show more solubility in toluene or benzene than in *n*-pentane or diethyl ether. Although these compounds are sensitive to moisture, they can be stored for months in an inert atmosphere without detectable decomposition.

Attempts to utilize reaction 1 for the synthesis of $Me_2NSn(HNCH_2CH_2)_3N$ (**13**) produced only nonvolatile, oligomeric/polymeric materials. We attribute this to the fact that the availability of a second reactive hydrogen on each primary nitrogen arm of tren allows elimination of additional $HNMe_2$ intermolecularly. After a reaction time of 3 h at 60 °C, only a ca. 10% yield of a white solid was obtained which was soluble in benzene. Although ^1H and ^{13}C NMR data[26] are consistent with the formation of a dimer structure **14**, no analytically pure compound

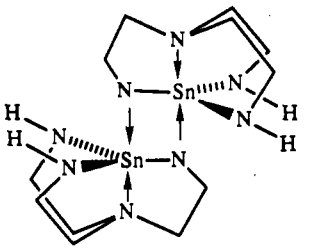

14

could be isolated. Support for the structure of **14** stems from the similar NMR spectra of the silicon analogue, which has been structured by X-ray means.[27]

When **11** is slowly hydrolyzed by atmospheric moisture the corresponding oxygen-bridged diazastannatrane **12** is formed (reaction 2). Attempts to perform this reaction by adding the stoichiometric amount of water diluted with THF to a toluene solution of **11** gave **12** in lower yields along with cage-opened products, as indicated by ^1H NMR spectra.

Spectroscopic Features. In all cases, molecular ion peaks (M^+) as well as $(M + H)^+$ peaks were observed in the high-resolution mass spectra (relative intensities: 0.1–7%), of which the M^+ peak was the dominant one. For compounds **5**, **7**, and **9**, which possess the Me-tren framework, the peak at m/e 305 (^{120}Sn), which is due to loss of the apical group Z, is usually the most abundant in the range $m/e > 100$.

From normal-coordinate analyses of silatranes (**1**, M = Si),[28,29] it is known that the vibrations for such cage compounds are highly mixed, and hence a desired assignment of the transannular bond to a single mode is impossible. Moreover, potential energy

(24) (a) Neutral-atom scattering factors and anomalous scattering corrections were taken from: *International Tables for X-ray Crystallography*; The Kynoch Press: Birmingham, England, 1974; Vol. IV. (b) Enraf-Nonius Structure Determination Package, Enraf-Nonius, Delft, Holland.
(25) Yoder, C. H.; Zuckerman, J. J. *J. Am. Chem. Soc.* **1986**, *88*, 4831.
(26) ^1H NMR (C_6D_6): δ 3.45 (t, 4H), 3.01 (m, 8H), 2.22 (m, 12H), 0.44 (s, broad, 4H). ^{13}C NMR (C_6D_6): δ 57.14, 53.98, 43.82, 39.29 (relative intensities 1:2:1:2).
(27) Wan, Y.; Verkade, J. G. In preparation.
(28) Imbenotte, M.; Palavit, G.; Legrand, P.; Hurenne, J. P.; Fleury, G. *J. Mol. Spectrosc.* **1983**, *102*, 40.
(29) Hencsei, P.; Sebestyén, A. *Main Group Met. Chem.* **1988**, *11*, 243.

Table V. ^{1}H NMR Data for Azastannatranes Z-Sn(NRCH$^1_2$CH$^2_2$)$_3$N **5–12**[a]

cmpd	δ(H^1)	δ(H^2)	^3J(H^{1}H^2)	R	δ(R)	^3J(H^{R}H^R)	Z	δ(Z)
5	2.75 (51.3)	2.29 (6.0)	5.7	Me	2.81 (49.2)		*n*-Bu	0.91 t, 1.14 (68.7) m, 1.40 tq, 1.80 m
6	2.94 (60.9)	2.28 (8.4)	5.4	H	0.23 (31.0)	3.7	*n*-Bu	0.72 (70.0) m, 0.86 t, 1.34 tq, 1.53 (75.0) m
7	2.73 (54.3)	2.26 (2.9)	5.6	Me	2.78 (51.8)		Me	0.37 (60.6)
8	2.91 (65.4)	2.20 (4.2)	5.4	H	0.20[b]	3.6	Me	0.02 (64.2)
9	2.78 (57.9)	2.22 (5.4)	5.4	Me	2.79 (54.3)		Ph	7.10–7.23 m, 7.92 (54.3) m[d]
10	2.88 (68.4)	2.15 (4.5)	5.4	H	0.40 (25.8)[c]	3.6	Ph	7.15–7.30 m, 7.66 (55.5) m[d]
11	2.72 (68.4)	2.11 (4.2)	5.7	Me	2.90 (54.0)		NMe$_2$	3.07 (43.5)
12	2.84 (78.6)	2.21[e]	5.5	Me	3.25 (55.8)			

[a] At 293 K in d$_6$-benzene-d_6; δ and *J* are given in ppm and Hz, respectively. ^{119}Sn–^{1}H coupling constants are given in parentheses (Hz). [b] Broad resonance, $\Delta\nu_{1/2}$ = 17 Hz. [c] At 243 K in d$_8$-toluene-d_8. [d] Meta–para and ortho hydrogens, respectively. [e] ^{119}Sn–^{1}H coupling not observed; $\Delta\nu_{1/2}$ = 3.6 Hz.

Table VI. Solid-State[a] and Solution[b] ^{13}C NMR Chemical Shifts (ppm) for Azastannatranes Z-Sn(NRC^{1}H$_2$C^{2}H$_2$)$_3$N **5–12**

	C^1			C^2			R			Z		
cmpd	δ$_{iso}$	δ(soln)	Δδ[c]	δ$_{iso}$	δ(soln)	Δδ[c]	δ$_{iso}$	δ(soln)	Δδ[c]	δ$_{iso}$	δ(soln)	Δδ[c]
5		49.8 (5.0)			50.4 (20.6)			40.8 (20.2)			11.5 (625)[e]	
6		39.0 (16.1)			53.5 (29.7)						17.0 (589)[f]	
7	46.1[d]	49.5 (7.6)	−3.4	46.1[d]	50.6 (19.8)	−4.5	38.6	40.0 (21.0)	−1.4	−10.9	−9.4 (601)	−1.5
8	39.1	39.0 (14.9)	0.1	57.2	53.4 (31.7)	3.8				−2.2	−4.2 (555)	2.0
9	48.6[d]	50.1 (8.1)	−1.5	48.6[d]	50.5 (27.7)	−1.9	*g*	41.0 (15.1)	−1.1/0.2		*h*	
10	*i*	38.9 (11.5)	−0.4/0.8	*j*	53.4 (33.8)	−0.5/3.2/5.3					*h*	
11	47.5[d]	50.1 (13.4)	−2.6	47.5[d]	50.3 (31.7)	−2.8	39.7	40.7 (4.8)	−1.0	42.2	44.0 (3.2)	−1.8
12	49.2[d]	49.9 (18.2)	−0.7	49.2[d]	50.8 (25.2)	−1.6	37.9	39.9 (6.0)	−2.0			

[a] δ$_{iso}$. [b] At 293 K. Solution data from benzene-d_6 solutions. ^{119}Sn–^{13}C coupling constants are given in parentheses (Hz). [c] δ(solid) − δ(soln). [d] Signal is 600 Hz broad. [e] Remaining ^{13}C: δ 28.5 (29.4), 28.2 (98.0), 13.9 (7.2). [f] Remaining ^{13}C: δ 28.9 (27.7), 27.6 (70.5), 14.1 (not obsd). [g] 39.9, 41.2 (2:1 ratio). [h] See Table VIII. [i] 38.5, 40.7 (1:1 ratio). [j] 52.9, 56.6, 58.7 (2:1:1 ratio).

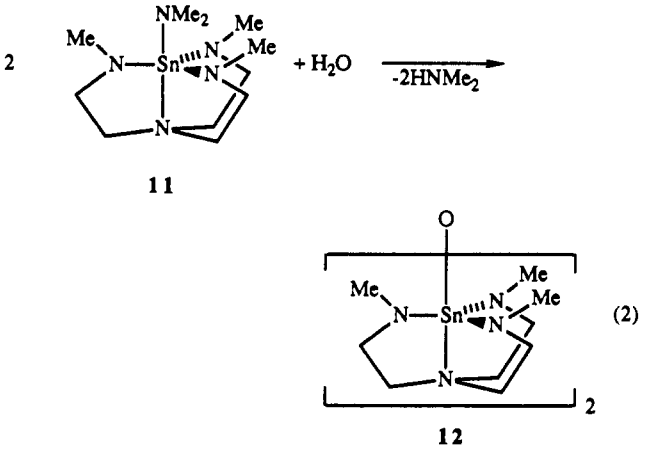

contributions from the Si–N$_{ax}$ bond stretching coordinate were attributed to different absorption bands. In force field calculations,[28,29] the band at 348 cm^{-1} was the only one consistently attributed to a Si–N$_{ax}$ bond stretching contribution and it was the only absorption band wherein this contribution was found to be dominant. Earlier, the absorption band at 348 cm^{-1} had been assigned as pure Si–N$_{ax}$ bond stretching in silatranes.[30] Assuming that the force field is similar, the mass change from silicon to tin would lead to a predicted absorption band around 300 cm^{-1} for a localized stretching mode. This is consistent with the observation of a weak absorption band between 288 and 307 cm^{-1} for all the azastannatranes discussed here. The absorption band at 484–495 cm^{-1} for stannatranes (**1**, M = Sn) assigned to Sn–N$_{ax}$ bond stretching[12b] is also found for these azastannatranes (491–521 cm^{-1}), and it may be attributable to a vibration with a potential energy contribution from the Sn–N$_{ax}$ bond stretching coordinate.

The ^{1}H, ^{13}C, and ^{119}Sn NMR data for compounds **5–12** are given in Tables V–VII. The AA′XX′ spectra for the methylene protons of the azastannatrane cage appear as two sets of virtual triplets, as has previously been observed for a variety of silatranes,[31] azasilatranes,[3b] and stannatranes.[11,12] In the cases of compounds **6**, **8**, and **10**, where a hydrogen is present at the equatorial nitrogens, an additional splitting of the nearby methylene protons appears.

Table VII. Solid-State and Solution[a] ^{119}Sn NMR Isotropic Chemical Shifts (ppm) for Azastannatranes **5–12**

cmpd	δ$_{iso}$(solid)	Δν$_{1/2}$(solid)[b]	δ(soln)	Δδ[c]
5			−117.1	
6			−69.5	
7	−91.8	110	−90.0	−1.8
8	−49.0	160	−57.5	8.5
9	−132.4	170	−150.6	18.2
10	−110.1 (Sn(1))[d]	230	−120.8	10.7
	−92.8 (Sn(2))[d]	230	−120.8	28.0
11	−171.0	230	−177.3	6.3
12	−254.0	410	−255.2	1.2

[a] At 293K. Solution data measured in d_6-benzene-d_6 solutions. [b] In Hz. [c] δ(solid) − δ(soln). [d] See Figures 3 and 4 for atom labeling.

The pentacoordinate nature of azastannatranes **5–11** (see later) is reflected in a decreased two- or three-bond *J*(^{119}SnH) value for the proton nearest to Sn in the apical group compared with the *J* values of similar tetracoordinated compounds: *ca.* 70 Hz for **5** and **6**, 72.0 Hz for *n*-BuSn(NMe$_2$)$_3$; *ca.* 64 Hz for **7** and **8**; 69.0 Hz for MeSn(NMe$_2$)$_3$; 43.5 Hz for **11**; 51.0 Hz for Sn(NMe$_2$)$_4$. These differences are consistent with less s character in the apical bond of the five-coordinate compounds and less positive charge on the tin atom. The ^{119}Sn–^{13}C coupling constant for the cage carbons bound to the axial nitrogen (20–32 Hz) is larger than the one for the carbons attached to the equatorial nitrogens (5–16 Hz). Further evidence for pentacoordination in azastannatranes is that their ^{119}Sn chemical shifts are all found in the high-field region characteristic for five-coordinate structures. For the substituted azastannatranes **6**, **8**, and **10**, comparison of the ^{119}Sn chemical shifts with those of the corresponding tris(dimethylamino)stannanes reveals a coordination chemical shift[32] of 30–45 ppm. *N*-Methyl substitution in azastannatranes causes pronounced upfield movements of the ^{119}Sn chemical shift of

(30) Anosov, V. P. Ph.D. Thesis, Moscow State University, Moscow, 1979. Referenced in: Hencsei, P.; Gál, M.; Bihátsi, L. *J. Mol. Struct.* **1984**, *114*, 391.

(31) Sidorkin, V. F.; Pestunovich, V. A.; Voronkov, M. G. *Magn. Reson. Chem.* **1985**, *23*, 491.

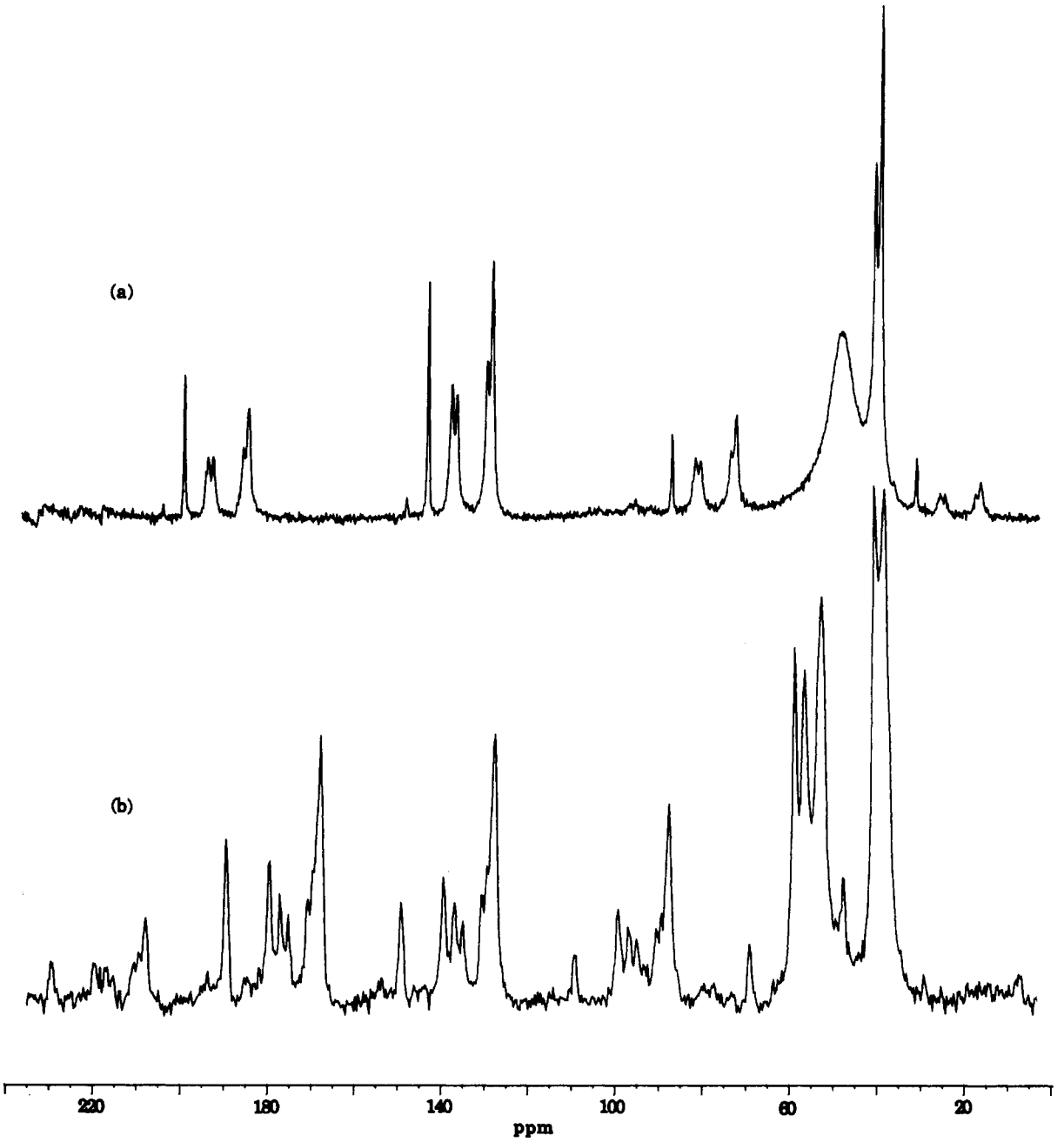

Figure 1. ^{119}Sn CP/MAS NMR spectrum of **11** obtained at 111.92 MHz with a spinning frequency of (a) 1402 Hz (2048 scans) and (b) 3496 Hz (400 scans).

Table VIII. ^{119}Sn Shielding Tensor Data (ppm) for Azastannatranes **7–12**[a]

cmpd	σ_{11}	σ_{22}	σ_{33}	δ_A[b]	η[c]	σ_{iso}
7	150	123	2	−90	0.30	91.8
8	136	94	−83	−132	0.32	49.0
9	242	186	−31	−163	0.34	132.4
10 (Sn(1))[d]	254	183	−107	−217	0.33	110.1
10 (Sn(2))[d]	264	136	−122	−215	0.60	92.8
11	300	220	−7	−178	0.45	171.0
12	386	340	36	−218	0.21	254.0

[a] The principal axes were chosen according to Haeberlen's notation,[34] where $|\sigma_{33} - \sigma_{iso}| \geq |\sigma_{11} - \sigma_{iso}| \geq |\sigma_{22} - \sigma_{iso}|$. [b] Anisotropy parameter $\delta_A = \sigma_{33} - \sigma_{iso}$. [c] Asymmetry parameter $\eta = (\sigma_{22} - \sigma_{11})/\delta_A$. [d] Figures 3 and 4 for atom labeling.

60–80 ppm. This behavior is opposite to that observed previously for azasilatranes.[3b]

The data obtained from solid-state NMR experiments are given in Tables VI–IX. High-resolution solid-state ^{119}Sn CP/MAS NMR spectroscopy has been shown to be an effective tool for the detection of even subtle details in the structural and electronic properties of organotin compounds.[33] As a manifestation of the three-dimensional nature of the chemical shielding, the spectrum of a stationary powder sample will show a chemical shift anisotropy pattern.[34] The singularities in this powder pattern correspond to the diagonal elements of the chemical shielding tensor in the principal-axis system (PAS). Magic-angle spinning at a speed below the powder line width causes the pattern to break up into an isotropic line (i.e., $\sigma_{iso} = {}^1/_3(\sigma_{11} + \sigma_{22} + \sigma_{33})$) flanked by spinning sidebands. The intensities of the spinning sidebands are related to the chemical shielding tensor and can be used to calculate its parameters by a graphical analysis.[35] As a typical example, the ^{119}Sn CP/MAS spectrum for **11** is shown in Figure 1. The chemical shielding tensor can be rewritten according to the

(32) $\delta\Delta$(coord) = δ(RSn(NMe$_2$)$_3$) − δ(azastannatrane).

(33) Apperley, D. C.; Davies, N. A.; Harris, R. K.; Brimah, A. K.; Eller, S.; Fischer, R. D. *Organometallics* **1990**, *9*, 2672 and references therein.
(34) Haeberlen, U. *High Resolution NMR in Solids*; Waugh, J. S., Ed.; Advances in Magnetic Resonance, Supplement 1; Academic Press: New York, 1976.
(35) Herzfeld, J.; Berger, A. E. *J. Chem. Phys.* **1980**, *73*, 6021.

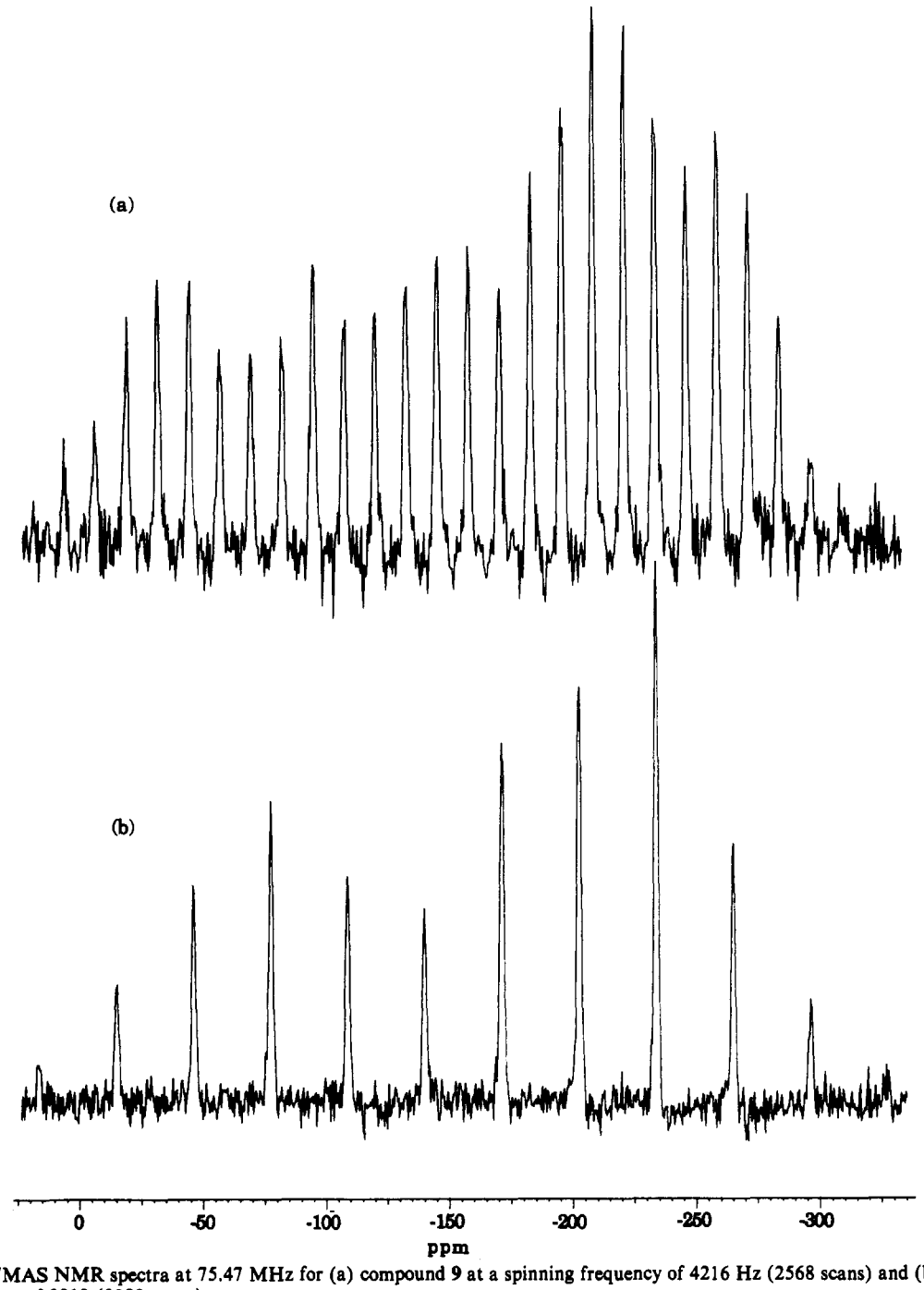

Figure 2. ^{13}C CP/MAS NMR spectra at 75.47 MHz for (a) compound **9** at a spinning frequency of 4216 Hz (2568 scans) and (b) compound **10** at a spinning frequency of 3010 (3208 scans).

definitions given in Table VIII,[34] thus providing a more suitable set of parameters (i.e., σ_{iso}, η the asymmetry parameter, and δ_A the anisotropy parameter) for comparison.

The rather moderate changes for the chemical shifts of −1.8 to +28.0 ppm for $\Delta\delta$ (see Table VII) in these azastannatranes from the solution to the solid state indicates that pentacoordination is maintained.[36] The solution chemical shifts are with one exception upfield with respect to the solid state, suggesting that the Sn–N_{ax} interaction may generally be stronger in solution (see later). The asymmetries η are, with one exception (**10**, η = 0.6), roughly 0.3, which indicates that the tensors are close to axial symmetry in these azastannatranes. Since the differences for the anisotropy of compounds **5–12** (δ_A = 90–218 ppm) are within the range observed for other tin species,[33] we attribute the variation in δ_A primarily to the changing nature of the apical substituents. The fact that in **10** two crystallographically different sites for tin are present was confirmed by its structure, which was determined by X-ray means (see later). The two molecules possess different Sn–N_{ax} bond distances (Sn(1)–N(1) = 238.0(2) pm, Sn(2)–N(5) = 245.3(2) pm), the shorter one of which is assigned to the sideband manifold with the isotropic chemical shift at higher field (δ_{iso} = −110.1 ppm), since a higher shielding is expected for the stronger donating interaction. The rather dramatic difference in the asymmetry in these two molecules (Sn(1), η = 0.33; Sn(2), η = 0.60) is in good agreement with the proposed assignment, since the structure shows a significant distortion from the expected axial symmetry only in the case of the molecule containing Sn(2). According to our ^{119}Sn CP/MAS data, all the other azastannatranes (**5–9**, **11**, and **12**) possess only one crystallographic site for their tin atoms.

The ^{13}C CP/MAS spectral data summarized in Table VI reveal chemical shifts similar to those in the solution spectra described above. The close chemical shifts for the two methylene cage carbons in the azastannatranes possessing the Me-tren framework

(36) Harris, R. K.; Sebald, A.; Furlani, D.; Tagliavini, G. *Organometallics* **1988**, *7*, 388.

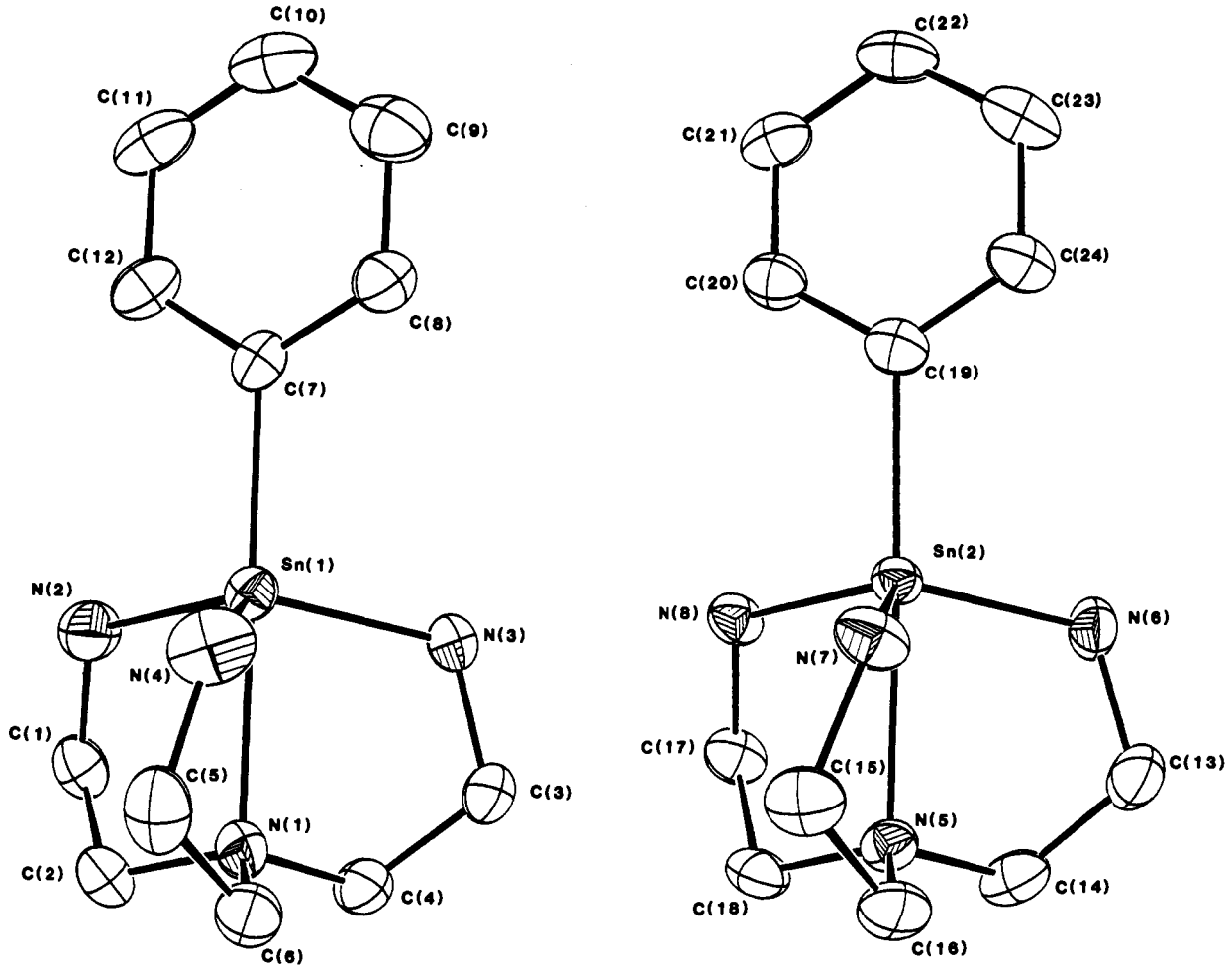

Figure 3. ORTEP drawing of both independent molecules of **10** with ellipsoids drawn at the 50% probability level.

Table IX. Solid-State and Solution ^{13}C NMR Data (ppm) for the Phenyl Groups in Azastannatranes **10** and **11**[a]

		σ_{11}	σ_{22}	σ_{33}	δ_A[b]	η[c]	δ_{iso}(solid)[d]	δ(soln)[d]	$\Delta\delta$[e]
9	ipso	−226	−193	−13	131	0.25	143.5 (732)	141.7 (784)	1.8
	ortho	−230	−144	−17	113	0.76	130.0	128.6 (62.9)	1.4
	meta	−245	−144	−21	116	0.87	136.9	138.1 (34.8)	−1.2
		−245	−147	−22	116	0.85	138.1		0.0
	para[f]	−231	−139	−17	112	0.82	128.6	128.7 (13.1)	−0.1
10	ipso	−238	−206	−3	146	0.22	149.1 (655)	146.9 (713)	2.2
	ortho	−221	−141	−21	106	0.75	127.6	128.4 (61.0)	−0.8
	meta	−225	−156	−25	110	0.63	135.0	136.0 (38.8)	−1.0
		−226	−157	−28	109	0.63	136.7		0.7
		−227	−161	−31	108	0.61	139.4		3.4
	para	−220	−144	−24	105	0.72	129.3	128.8 (12.9)	0.5
		−221	−145	−26	105	0.72	130.6		1.8

[a] The principal axes were chosen according to Haeberlen's notation;[34] see Table VII. [b] Anisotropy parameter. [c] Asymmetry parameter. [d] ^{119}Sn–^{13}C coupling (Hz) constant in parentheses. [e] δ(solid) − δ(soln). [f] Overlapped with the second ortho resonance; therefore the tensor data cannot be assigned to either carbon.

gave rise to only one peak with a half-height width of 600 Hz, whereas the other resonances are sharp and resolved. For compound **10**, the existence of two crystallographically different azastannatrane units is also reflected in its ^{13}C CP/MAS NMR spectrum (Figure 2). The assignments of the phenyl carbons in **9** and **10** (Table VIII) are suggested by their similarity to those in solution and are supported by similar asymmetry parameters η for corresponding carbons. Not unexpectedly, the ipso carbons in **9** (η = 0.25) and **10** (η = 0.22) both show rather high axial symmetry. Furthermore, the one-bond ^{119}Sn–^{13}C coupling that is observed in both cases is about the same as that observed in solution. The ^{13}C CP/MAS NMR spectrum of **9** (Figure 2) shows two sharp resonances for the methyl carbons. This can be rationalized if the phenyl ring in the molecule is oriented coplanar

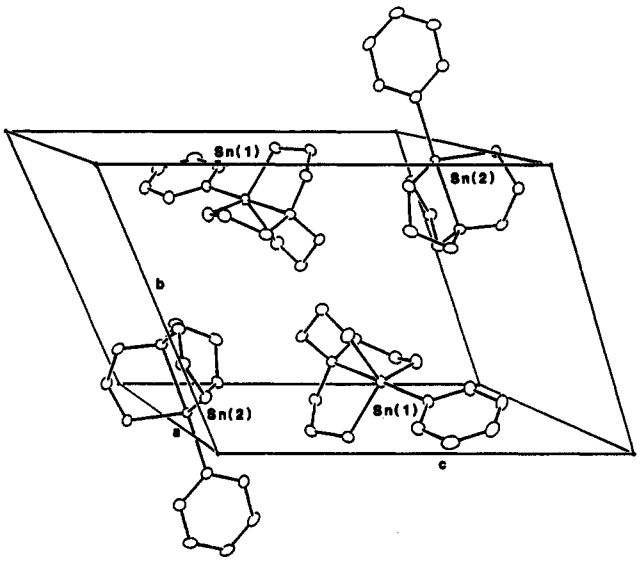

Figure 4. Unit cell drawing for the structure of **10** with only the tin atoms numbered.

with or perpendicular to one of the three N_{eq}–Sn–N_{ax} planes, respectively. Because of the observation of two different meta and ortho carbon ^{13}C resonances, we tend to favor the coplanar conformation even though such an eclipsed conformation would seem less favored sterically.

Crystal and Molecular Structure of 1-Phenylazastannatrane (10). The X-ray crystallographic study of **10** revealed the presence of two crystallographically independent molecules (Figure 3). In both molecules, the tin atoms possess a trigonal bipyramidal coordination sphere (axial angles of tin: N(1)–Sn(1)–C(7) = 178.75(9)°; N(5)–Sn(2)–C(19) = 177.43(9)°) similar to that in

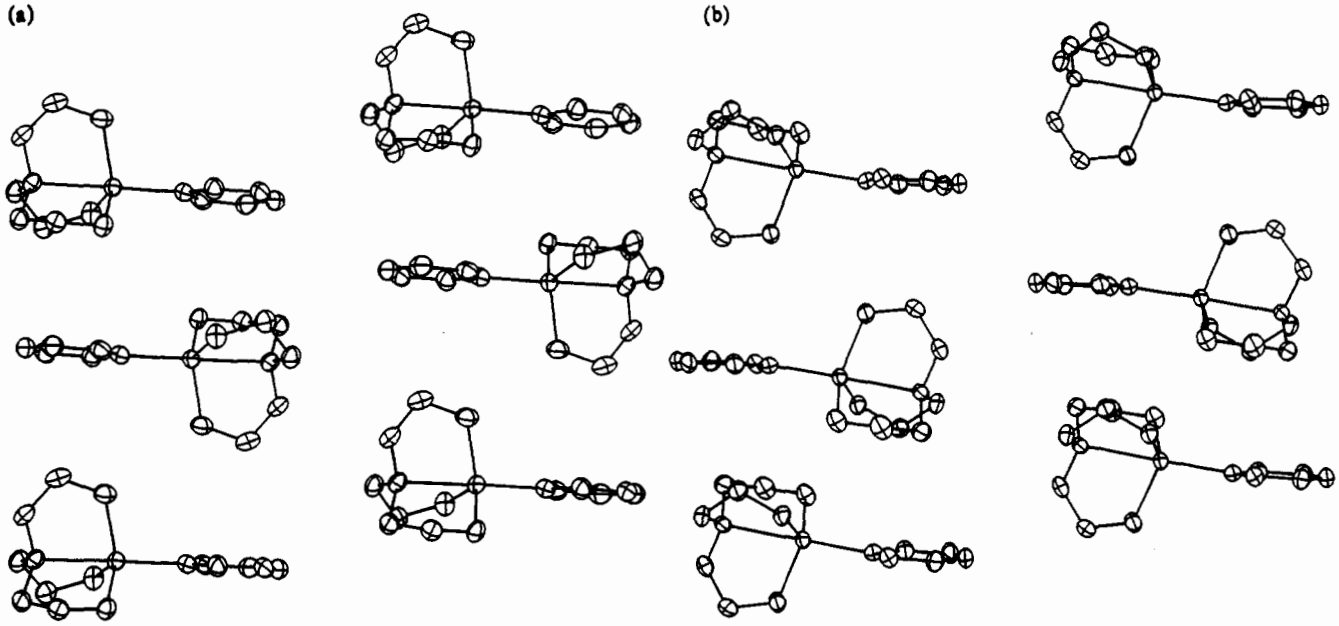

Figure 5. Array of molecules containing (a) Sn(1) and (b) Sn(2), respectively. The view is parallel to normal vector of the *ab* plane.

azasilatranes[3b] and stannatranes.[11e] The only significant differences between these two molecules are the two axial bond lengths at the tin (Sn(1)–N(1) = 238.0(2) pm; Sn(2)–N(5) = 245.3(2) pm) and the angle between the phenyl ring plane and the tin–(ipso) carbon bond vector (Sn(1)–C(7) = 179.1(2)°; Sn(2)–C(19) = 173.2(2)°). Both observed Sn–N_{ax} bond distances are in the lower part of the range known for tin–nitrogen interactions in five-coordinate organotin compounds (232–266 pm).[11d] The equatorial Sn–N bond distances in **10** (average 205.8(2) pm) compare very well to that found for a Sn–N single bond (206 ± 4 pm).[37] The N_{ax}–Sn–N_{eq} angles (average 77.8(8)°) are about 5° smaller than those found in azasilatranes,[3b] which might be attributed to the larger covalent radius of tin.

The arrangement of the molecules in the unit cell is given in Figure 4. The structure is composed of two different layers of antiparallel stacks of azastannatrane molecules, containing Sn(1) and Sn(2), respectively. These layers form sheets (Figure 5) coplanar to the plane given by *a* and *b*, which are then packed along the *c* direction. Figure 5 shows the basic difference in the packing of those two types of sheets. The bending of the phenyl rings in the molecule containing Sn(2) seems to be due to an avoided intermolecular contact between the corresponding phenyl rings (see Figure 5). The substantial difference between the two Sn–N_{ax} bond lengths (7.3 pm) suggests the possibility of a rather flat potential surface for the Sn–N_{ax} interaction, since this bond length differential was imposed by what appear to be moderate differences in packing.

Azastannatrane Framework Racemization. The two most interesting features of atrane frameworks are their transannular interactions and the racemization of their chiral molecular skeletons. The ^{1}H spectra of **5–11** upon cooling below 198 K show strong broadening for the two methylene proton triplets, which eventually split again into two broad singlets. All the other resonances remain sharp and well resolved down to 163 K. This behavior is indicative of a racemization process.[38] The ΔG_{Tc}^* of activation values for racemization, calculated from the coalescence of the methylene protons adjacent to the axial nitrogen, are summarized in Table X.

Table X. ΔG_{Tc}^* (kJ/mol) for the Racemization of the Azatrane Frameworks in Azastannatranes **5–11**[a]

	T_c[b]	$\Delta\nu$[c]	ΔG_{Tc}^*[d]		T_c[b]	$\Delta\nu$[c]	ΔG_{Tc}^*[d]
5	176	210	33.3	**9**	180	143	34.7
6	193	251	36.4	**10**	178	225	33.6
7	181	166	34.7	**11**	178	150	34.2
8	190	256	35.8				

[a] Calculated from coalescence of the $N(CH_2)_3$ proton resonance in toluene-d_8. [b] T_c in K. In all cases the toluene-d_8 solution could be supercooled down to 163 K. [c] $\Delta\nu$ in Hz. [d] ±0.3 for ΔT_c = 1 K, $\Delta(\Delta\nu)$ = 10 Hz.

A comparison of ΔG_{Tc}^* values for analogues containing the tren and Me-tren frameworks (i.e., Z = Me and *n*-Bu) reveals that the unsubstituted (tren) skeleton seems to be less rigid, whereas for Z = Ph both analogues display values within the margin of error. The conclusion of Tzschach et al. that ΔG_{Tc}^* for racemization of tricarbastannatranes **3** is independent of the strength of the Sn–N_{ax} interaction[38] is consistent with our findings for azastannatranes. For tricarbasilatranes (**3**, M = Si) the racemization barrier is about the same (34.7 kJ/mol)[38] as in compounds **5–11**, but in tricarbastannatranes it is somewhat higher (37.2–37.8 kJ/mol).[38] This suggests that the barrier for racemization of the chiral atrane skeleton is mainly dependent upon the central element M and the nature of the equatorial groups, not on the strength of the M–N_{ax} interaction.

Acknowledgment. The authors thank the Deutsche Forschungsgemeinschaft for a Postdoctoral Fellowship to W.P., the NSF and the AFOSR for grant support of this research, the W. R. Grace Co. for a research sample of tren, and Dr. Lee Daniels of the Iowa State Molecular Structure Laboratory for the X-ray structure determination of **10**.

Supplementary Material Available: Text giving elemental analyses and mass and infrared data and for **10** tables of positional and isotropic thermal parameters for H atoms anisotropic thermal parameters (11 pages). Ordering information is given on any current masthead page.

(37) Alcock, N. W.; Pierce-Butler, M.; Willey, G. R.; Wade, K. *J. Chem. Soc., Chem. Commun.* **1975**, 183.
(38) Mügge, C.; Pepermans, H.; Gielen, M.; Willem, R.; Tzschach, A.; Jurkschat, K. *Z. Anorg. Allg. Chem.* **1988**, *567*, 122.